DESIGN AND MODELING OF A COMPTON-SUPPRESSED PHOSWICH DETECTOR FOR RADIOXENON MONITORING

Abi T. Farsoni and David M. Hamby

Oregon State University

Sponsored by the National Nuclear Security Administration

Award No. DE-AC52-09NA29324
Proposal No. BAA09-27

ABSTRACT

By measuring the concentration of four xenon radioisotopes in the atmosphere, the International Monitoring System (IMS) can verify nuclear weapons tests around the world. To measure ultra-low concentrations of radioxenons, many detection systems, such as the Automated Radioxenon Sampler and Analyzer (ARSA) and the Swedish Automatic Unit for Noble gas Acquisition (SAUNA), have been developed and are currently under field tests. These systems employ the beta/gamma coincidence technique to facilitate background rejection. Since all of these systems use two separate detection systems for detecting beta-particles and gamma-rays, the calibration process is usually a tedious task. A phoswich detector, however, can simplify radioxenon detection by measuring both radiations with a single detector.

A phoswich detector with Compton suppression capability for measuring xenon radioisotopes has been designed and simulated. The expected performance of the phoswich detector in suppressing Compton interactions and shielding against background radiation was modeled using MCNPX Version 2.5.0. The Compton suppression mechanism is integrated into the phoswich design to effectively reduce the Compton continuum in 2D gamma/beta coincidence spectra and significantly improve the Minimum Detectable Concentration (MDC) of the xenon radioisotopes. The phoswich detector has been designed with three scintillation layers: a thin plastic scintillator layer to detect beta and conversion electrons, a CsI(Tl) crystal layer for detecting X-rays and gamma-rays and a BGO crystal, which surrounds the CsI(Tl) layer, to identify scattered photons and to shield the CsI(Tl) crystal against external gamma-ray background.

OBJECTIVE

The measurement of radioactive xenon in atmosphere is one of the major techniques employed for monitoring underground nuclear explosion. For compliance with the Comprehensive Nuclear-Test-Ban Treaty (CTBT), the International Monitoring System (IMS) will deploy sensitive automated radioxenon detectors at certain stations around the world to monitor the four xenon radioisotopes: ^{131m}Xe ($\tau_{1/2}$ = 11.9 day), ^{133m}Xe ($\tau_{1/2}$ = 2.2 day), ^{133}Xe ($\tau_{1/2}$ = 5.2 day), and ^{135}Xe ($\tau_{1/2}$ = 9.1 hour).

Within only a few years in the mid-1990s, four automated radioxenon measurement systems have been developed to fulfill the requirements of IMS stations: ARIX (Russia), ARSA (USA), SAUNA (Sweden), and SPALAX (France). In these systems, the atmospheric radioxenon concentration is measured either using high-purity germanium (HPGe) detector (SPALAX) or by a beta/gamma coincidence detection system as deployed in ARIX, ARSA and SAUNA. The systems that use beta/gamma coincidence technique are designed with two separate radiation detection channels: a NaI(Tl) scintillator for detecting gamma-rays and a plastic scintillator for detecting beta-particles (McIntyre et al., 2001). To provide minimal attenuation for beta-particles before they get detected, the gas cell in these systems is made of a plastic scintillator (beta detector). In the beta/gamma coincidence measurements, a two-dimensional beta/gamma coincidence spectrum is updated when the beta and gamma detectors are triggered within a fixed time window. The concentration of xenon radioisotopes then can be calculated through regions of interest corresponding to the four xenon radioisotopes in the 2D spectrum.

An alternative solution to measure beta/gamma coincidence events from radioactive xenon is to use phoswich detectors (Hennig et al., 2005; Farsoni et al., 2009) in which more than one scintillation layer is optically coupled to a single photomultiplier tube (PMT). To facilitate the pulse shape discrimination process in phoswich detectors (usually using digital pulse shape analysis), scintillators are selected from among those materials that have sufficient different decay times. In these detectors, a fast plastic scintillator is used for measuring beta-particles whereas a more dense and slower scintillator, such as NaI(Tl) or CsI(Tl), is used to detect gamma-rays.

In this work, a phoswich detector with Compton suppression capability has been designed and modeled to enhance the radioxenon measurements. Without using a secondary detector, the Compton suppression mechanism is integrated into the phoswich design to effectively reduce the Compton continuum in 2D gamma/beta coincidence spectra and significantly improve the Minimum Detectable Concentration (MDC) of the xenon radioisotopes. The expected performance of the phoswich detector in suppressing Compton interactions and shielding against background radiation was modeled using MCNPX Version 2.5.0.

RESEARCH ACCOMPLISHED

Compton Suppression Mechanism and Detector Design

In a beta/gamma coincidence detection system such as the ARSA system, as depicted in Figure 1, a two-dimensional beta/gamma coincidence spectrum is constructed to measure xenon radioisotopes. There are three boxed areas (in the absence of any radon daughters) from which the concentration of four xenon radioisotopes can be calculated. These areas are located at three gamma/x-ray energies; 30, 80, and 250 keV.

Although employing the beta/gamma coincidence measurement technique significantly increases the sensitivity of the detection system and improves the measurement of ultra-low radioactivity such as atmospheric isotopes of radioxenon in a high background field, there is still some probability for high-energy gamma-rays to be scattered through Compton scattering in the gamma detector. These interactions will add unwanted background for regions of interest at lower energies, e.g., at 30, 80, and 250 keV gamma-ray lines, in the two-dimensional beta/gamma spectrum. For instance, some of these coincidence events are indicated by a white arrow in Figure 1.
The high-energy gamma-rays could originate from either external or internal (from radon daughters or radioxenon itself in the gas sample) gamma-ray sources. These events will ultimately reduce sensitivity of the detection system and increase the MDC of radioxenon (McIntyre et al., 2006).

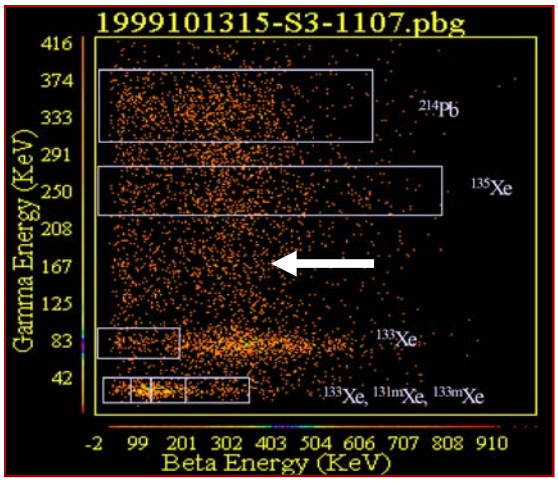

Figure 1. Two-dimensional beta/gamma spectrum from the ARSA system (taken from McIntyre et al., 2006). A white arrow in this Figure shows coincidence events recorded from beta absorption in the plastic scintillator and Compton scattering from higher energies (e.g., 250 keV from ^{135}Xe or 352 keV from ^{214}Pb) in the NaI(Tl) detector of the ARSA system.

The main objective of this research is to integrate an active Compton suppression mechanism into the phoswich design to further advance radioxenon detection and measurement by reducing the Compton background in the regions of interest of gamma-ray spectra. This feature will not require a secondary detector, sensor, electronics or additional photomultiplier tube. Figure 2 shows the schematic diagram of the phoswich detector. In this paper, we will call this detector an Actively-Shielded Phoswich (ASP) detector.

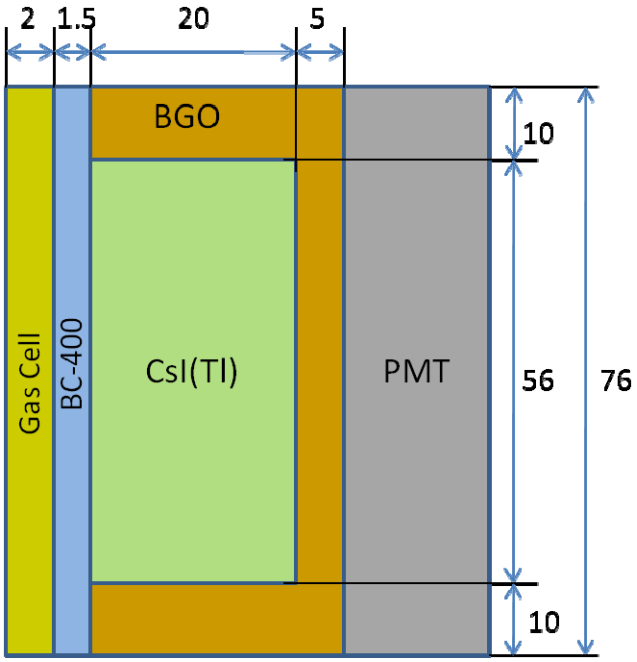

Figure 2. Schematic diagram of ASP detector designed to reduce Compton continuum in the regions of interest and shield the gamma detector against background radiation. All dimensions are in millimetres.

The ASP detector has been designed with three scintillation layers (see Figure 2): a thin plastic scintillator layer, BC-400, to detect beta and conversion electrons, a CsI(Tl) crystal layer for detecting X-rays and gamma-rays and a BGO crystal, which surrounds the CsI(Tl) layer, to identify scattered photons and to shield the CsI(Tl) crystal against external background gamma-rays. The BGO crystal is a high-density (7.13 g/cm^3) and high-efficient scintillator and is commonly used in Compton suppression systems. We integrate this crystal into our phoswich detector to identify unwanted Compton scatters from internal and external gamma-ray sources which could generate background into the beta/gamma coincidence spectra. Since the scintillation photons generated in this layer will be collected by the same PMT used for the other two layers, no additional light sensor or PMT is required for this task. The decay time of BGO crystal (300 nsec) is quite different from the other two scintillators (2.4 nsec of BC-400 and ~1,000 nsec of CsI(Tl)); this will facilitate our digital pulse shape analysis algorithm in discriminating the origin of radiation interactions.

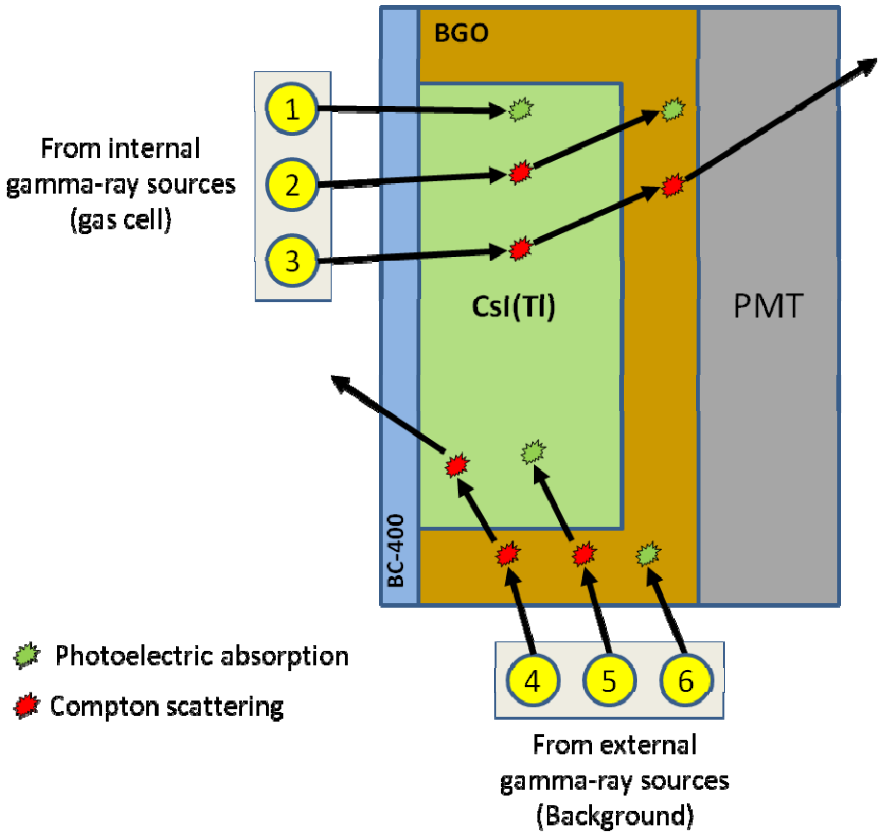

Figure 3. Major interaction scenarios in the ASP detector from internal and external gamma-ray sources. When accompanied with a coincident beta absorption in plastic scintillator, interaction scenarios 2 and 3 generate coincident pulses which are most likely responsible for Compton background in the two-dimensional beta/gamma coincidence spectrum. Corresponding pulses will be identified and rejected in our digital pulse processor (anti-coincidence logic).

Major interaction scenarios in the ASP detector from internal and external gamma-ray sources are illustrated in Figure. 3. Photons emitted from the sample source in scenarios 1, 2, and 3 are assumed to be coincident with a beta absorption in the plastic scintillator. In scenario 1, a gamma-ray from the sample source undergoes a photoelectric interaction and is fully absorbed in the CsI(Tl) crystal. If the resulting slow pulse is accompanied with a fast component from the plastic scintillator, the pulse will be identified as a valid beta/gamma coincidence event and the corresponding energy bin will be recorded in the 2-dimensional energy spectrum. A single gamma-ray may also generate such a coincidence pulse when it is fully absorbed in the CsI(Tl) after an scatter in the plastic scintillator. Since the plastic has a low Z and is very thin, the probability of this event is low. These mischaracterized events,

however, will form a diagonal line in the 2-D spectrum and therefore can be easily identified. In scenarios 2 and 3, a gamma-ray from the source is scattered in the CsI(Tl) crystal and will be either absorbed or scattered in the BGO crystal. When accompanied with a coincident beta absorption in plastic scintillator, interaction scenarios 2 and 3 generate coincident pulses which are most likely responsible for Compton background in the two-dimensional beta/gamma coincidence spectrum. These events can be identified and rejected (suppressed) by our digital pulse shape analysis (anti-coincidence logic).

One other advantage of using a BGO crystal in the ASP detector is to shield the CsI(Tl) crystal from background sources. Scenarios 4, 5, and 6 in Figure 3 show some events in which external gamma-rays from background radiation interact with the ASP detector. In scenarios 4 and 5, a gamma-ray from the external source is scattered in the BGO crystal and will be either absorbed or scattered in the CsI(Tl) crystal. In scenario 6, with no scattering, the external gamma-ray is fully absorbed in the BGO crystal. Pulses resulted from these scenarios will be rejected and will not contribute into the 2D energy spectra.

DETECTOR MODELING

The anti-coincidence feature of the MCNPX Version 2.5.0 was used to study the Compton suppression capability of the ASP detector. This study focuses on the evaluation of Compton suppression on three regions of interest of gamma-ray spectra for measuring the xenon radioisotopes. These regions are 30 keV X-ray, 81 keV, and 250 kev gamma-rays and are indicated by ΔE(30 keV), ΔE(81 keV) and ΔE(250 keV) in Figures 4-7. Approximately, one FWHM of these gamma-ray lines in the CsI(Tl) crystal were used to define these regions (Hennig et al, 2005, 2007, and 2008). Ranges for these regions of interest were 25-35 keV, 73-89 keV and 228-272 keV, respectively. The green distribution in Figures 4-7 shows the energy absorption in CsI(Tl) crystal with no event rejection (unsuppressed). The blue distribution shows the energy absorption in CsI(Tl) crystal when no energy absorption in the BGO crystal has been detected in coincidence with the CsI(Tl) crystal (suppressed).

For modeling the internal sources in Figures 4-7, three gamma-ray sources were used: ^{135}Xe (250 keV), ^{214}Pb (351.9 and 295.1 keV), and ^{214}Bi (609.3 keV). 250 keV from ^{135}Xe scattered in the CsI (Tl) crystal can generate Compton background in 30 and 81 keV regions. The two later sources, ^{214}Pb and ^{214}Bi, are two ^{222}Rn daughters which are readily observed by the beta/gamma counting systems. These beta-decaying isotopes emit high-energy gamma-rays (in coincidence with beta-particle) and are mainly responsible for Compton continuum in those three regions of interest (Bowyer et al., 1999). In Figures 4-6, a peak at about 74 keV in CsI(Tl) spectrum is observed. This peak is believed to be a characteristic X-ray of bismuth emitted after a photoelectric absorption in the BGO crystal.

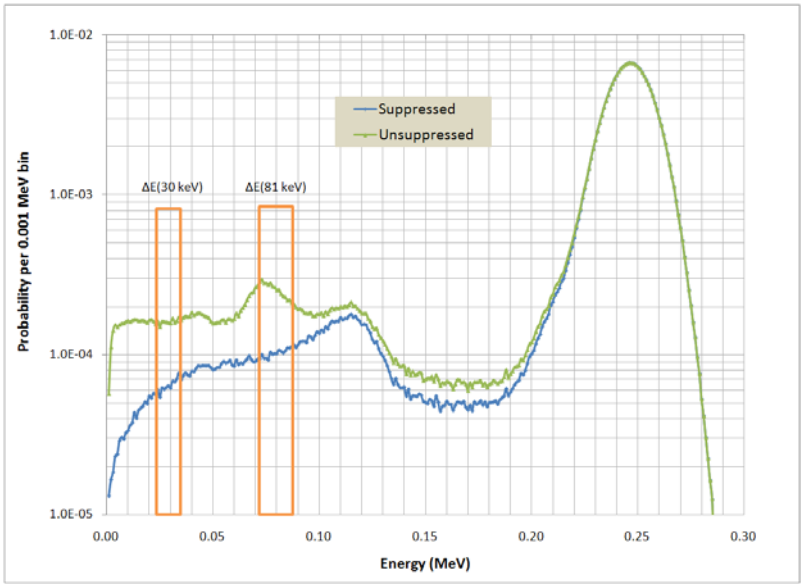

Figure 4. Suppressed and unsuppressed energy deposition spectra in CsI(Tl) crystal from 250 keV gamma-ray (from ^{135}Xe) modeled using the MCNPX.

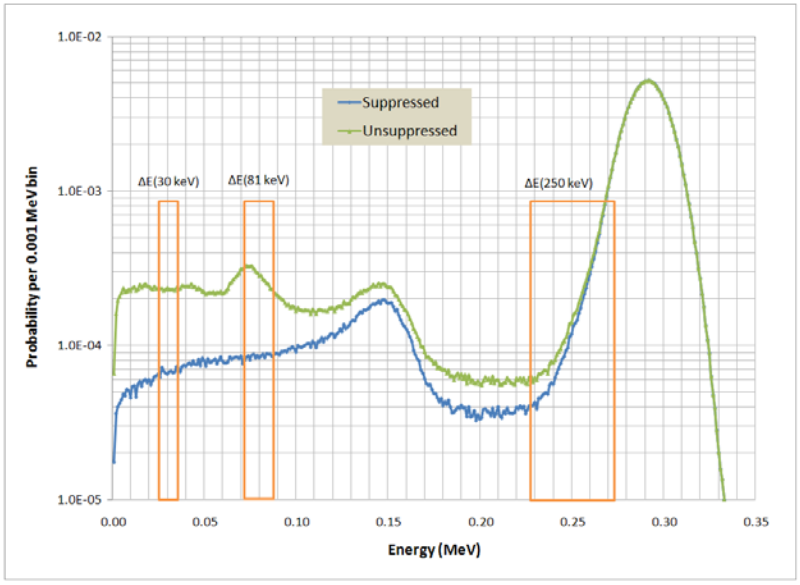

Figure 5. Suppressed and unsuppressed energy deposition spectra in CsI(Tl) crystal from 295.1 keV gamma-ray (from ^{214}Pb, a Radon daughter) modeled using the MCNPX.

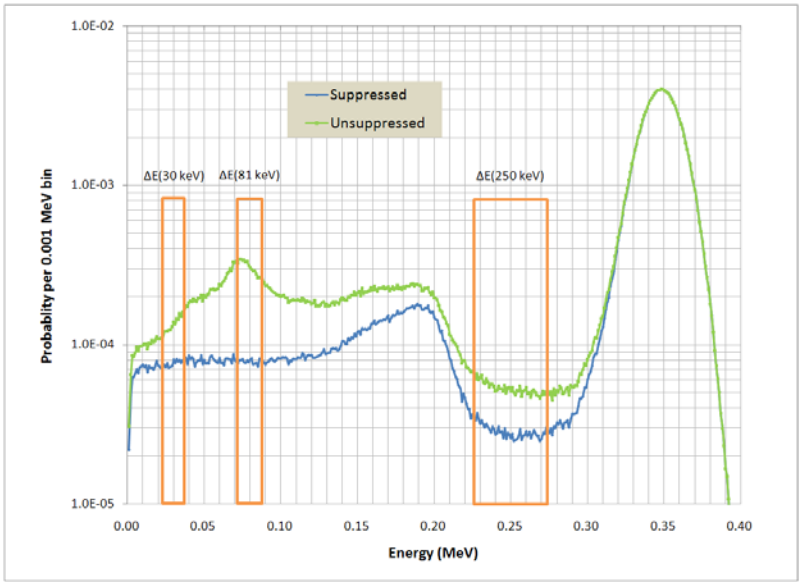

Figure 6. Suppressed and unsuppressed energy deposition spectra in CsI(Tl) crystal from 351.9 keV gamma-ray (from ^{214}Pb, a Radon daughter) modeled using the MCNPX.

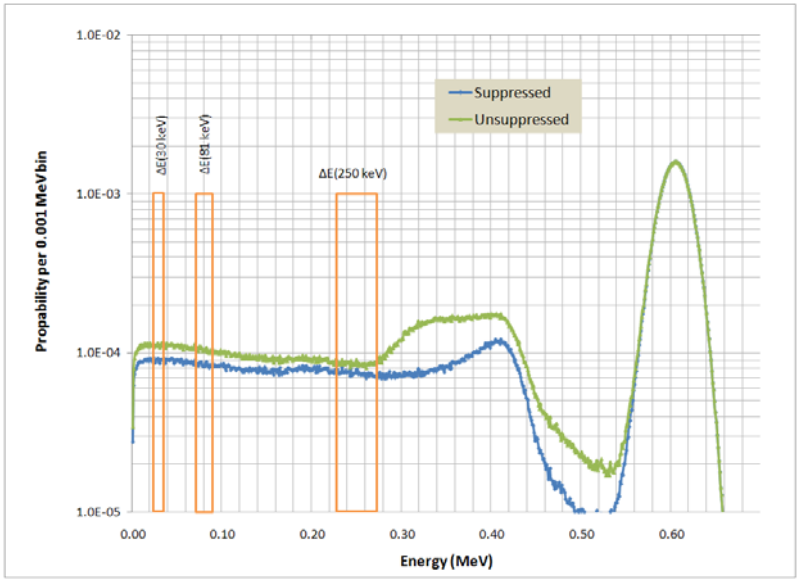

Figure 7. Suppressed and unsuppressed energy deposition spectra in CsI(Tl) crystal from 609.3 keV gamma-ray (from ^{214}Bi, a Radon daughter) modeled using the MCNPX.

The figure of merit used to measure the efficiency of the modeled suppression performance for each region of interest is the suppression factor, defined by:

$$\text{Suppression Factor} = \frac{\varepsilon_u(\Delta E) - \varepsilon_s(\Delta E)}{\varepsilon_u(\Delta E)} \times 100$$

where:

$\varepsilon_u(\Delta E)$ is the efficiency of events in the energy range of ΔE without using suppression (suppressed spectrum)

$\varepsilon_s(\Delta E)$ is the efficiency of events in the energy range of ΔE using suppression (unsuppressed spectrum)

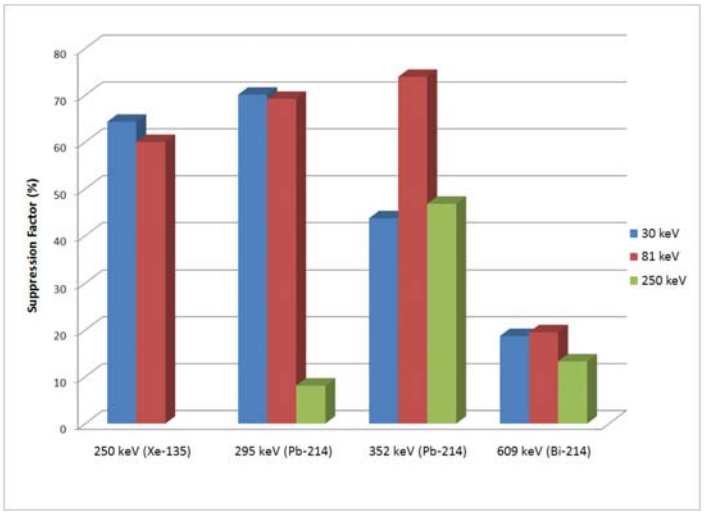

Figure 8. Suppression Factor in energy deposition spectra in CsI(Tl) crystal for three regions of interest from 250 keV, 295 keV, 352 keV and 609.3 keV gamma-rays modeled using the MCNPX.

The suppression factors calculated from four gamma-ray energy spectra given in Figures 4-7 are illustrated in Figure 8. As predicted in this Figure, for example, the Compton suppression mechanism integrated in the ASP detector reduces the Compton background in 30 keV and 81 keV regions (due to 250 keV gamma-rays from ^{135}Xe) by a factor of 64.3% and 60.0%, respectively. This factor is maximum (73.9%) for suppressing the Compton background at 81 keV region from 352 keV of ^{214}Pb. As expected, the suppression factor for all regions is dropped (13% to 20%) for high-energy gamma-rays from ^{214}Bi (609 keV), a daughter of radon.

To evaluate the phoswich detector in shielding against external sources (ambient background), a 2-mm disk source (1,460 keV from ^{40}K) was modeled on the back side of the detector, where the PMT is located in Figure 1. The source emits gamma-rays only in parallel with the detector axis. To study the effect of BGO layer in shielding the CsI (Tl) crystal against the background radiation, two simulations were performed with this high-energy gamma-ray source: (1) with BGO crystal as depicted in Figure 1, and (2) with BGO replaced by air. Figure 9 shows the results of these simulations. The green spectrum shows the energy deposition in CsI(Tl) crystal when the BGO crystal was replaced by air. The blue and red spectra are suppressed and unsuppressed energy spectra in CsI (Tl) crystal, respectively, when the phoswich was modeled with the BGO crystal. In addition of single- and double-escape peaks in these spectra, the unsuppressed energy spectrum with the BGO crystal (red spectrum) shows a significant peak at the Compton edge. This peak does not appear in the suppressed spectrum. Considering a non-isotropic source used in this simulation, low-angle scattered photons from the BGO crystal have a more chance to be absorbed in the CsI(Tl) crystal and therefore it might be a reason to have a pronounced Compton edge in the unsuppressed spectrum. Our calculations from this modeling show that the BGO layer (5 mm, at the back side) reduces the total efficiency of CsI(Tl) crystal in absorbing 1,460 keV from ^{40}K as much as 51.2%, when the suppressed (blue) spectrum is used. This is only 38.7% reduction when the unsuppressed (red) spectrum is used.

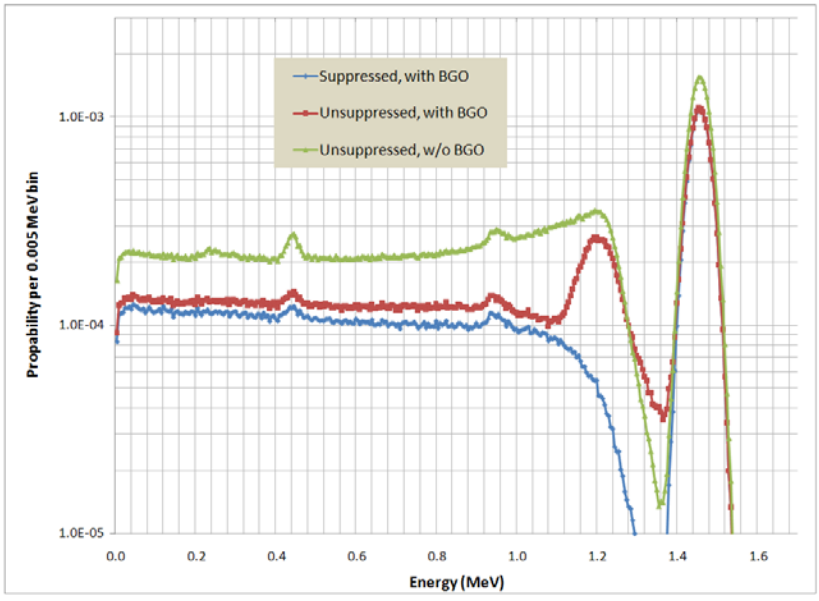

Figure 9. Energy deposition spectra in CsI(Tl) crystal from a ^{40}K external source. The blue and red spectra are suppressed and unsuppressed energy spectra, respectively, when the phoswich was modeled with the BGO crystal. The green spectrum was obtained when the BGO crystal was replaced by air.

A prototype detector with dimensions illustrated in Figure 1 is currently under construction. To have more flexibility in testing the detector with different PMT's, this detector is planned to be assembled in our laboratory. To do so, the required scintillation crystals have been ordered through the Saint-Gobain company. Due to their long lead-time, the prototype detector was not ready when this paper was prepared for publication. Other geometry designs such as well-type or two-channel versions, however, will be considered after our preliminary experiments with this simpler design.

CONCLUSION

The expected performance of a phoswich detector in suppressing Compton interactions was modeled using anti-coincidence feature of the MCNPX Version 2.5.0. The Compton suppression mechanism is integrated into the phoswich design to effectively reduce the Compton continuum and improve the Minimum Detectable Concentration (MDC) in measuring xenon radioisotopes. The phoswich detector has been designed with three scintillation layers: a thin plastic scintillator layer (coated with a 1-μ aluminum layer to minimize the memory effect) to detect beta and conversion electrons; a CsI(Tl) crystal for detecting X-rays and gamma-rays; and a BGO crystal, which surrounds the CsI(Tl) layer, to identify scattered photons and to shield the CsI(Tl) crystal against ambient background. Our modeling shows that when the phoswich detector is exposed to a gamma source of 250 kev from ^{135}Xe, the Compton suppression mechanism reduces the Compton background in 30 keV and 81 keV regions by a factor of 0.64 and 0.60, respectively. This factor is about 0.74 in 81 keV region when the detector is exposed to a gamma source of 352 keV from ^{214}Pb. Our modeling also predicts that the BGO layer (5 mm, at the back side of detector) reduces the total efficiency of CsI(Tl) crystal in absorbing 1,460 keV from ^{40}K as much as 51.2%, when the suppressed spectrum (anti-coincidence logic between pulses from CsI(Tl) and BGO crystals) is used.

REFERENCES

Bowyer, T. W., J. I. McIntyre, P. L. Reeder (1999). High-sensitivity detection of xenon isotopes via beta-gamma coincidence counting, in Proceeding of the 21st Seismic Research Review: *Ground-Based Nuclear Explosion Monitoring Technologies*, LA-UR-99-4700, Vol. 2, pp. 231–241.

Farsoni, A. T., D. M. Hamby (2009). Characterization of triple-layer phoswich detector for radioxenon measurements, in *Proceedings of the 2009 Seismic Research Review: Ground-Based Nuclear Explosion Monitoring Technologies*, LA-UR-09-05276, Vol. 2, pp. 631–640.

Hennig, W., H. Tan, W. K. Warburton, and J. I. McIntyre (2005). Digital pulse shape analysis with phoswich detectors to simplify coincidence measurements of radioactive xenon, in *Proceedings of the 27th Seismic Research Review: Ground-Based Nuclear Explosion Monitoring Technologies,* LA-UR-05-6407, Vol. 2, pp. 787–794.

Hennig, W., H. Tan, W. K. Warburton, A. Fallu-Labruyere, K. Sabourov, J. I. McIntyre, M. W. Cooper, and A. Gleyzer (2007). Characterization of phoswich well detectors for radioxenon monitoring, in *Proceedings of the 29th Monitoring Research Review: Nuclear Explosion Monitoring Technologies,* LA-UR-07-5613, Vol. 2, pp. 757–763.

Hennig, W., H. Tan, W. Warburton, A. Fallu-Labruyere, K. Sabourov, M. Cooper, J. McIntyre, and A. Gleyzer (2008). Development of a COTS Radioxenon Detector System Using Phoswich Detectors and Pulse Shape Analysis, in *Proceedings of the 30th Monitoring Research Review: Ground Based Nuclear Explosion Monitoring Technologies*, LA-UR-08-05261, Vol. 2, pp. 758–767

McIntyre, J. I., K. H. Able, T. W. Bowyer, J. C. Hayes, T. R. Heimbigner, M. E. Panisko, P. L. Reeder, R. C. Thompson (2001). Measurements of ambient radioxenon levels using the automated radioxenon sampler/analyzer (ARSA), *J. of Radioanalytical and Nuclear Chemistry*, 248: (3)629–635.

McIntyre, J. I., T. W. Bowyer, P. L. Reeder (2006). Calculation of minimum detectable concentration levels of radioxenon isotopes using the PNLL ARSA system, Technical Report, PNNL-13102.